Isogeometric Analysis and Symmetric Galerkin BEM: a 2D Numerical Study

Isogemetric Analysis and Symmetric Galerkin BEM: a 2D numerical study

A. Aimi[a,*], M. Diligenti[a], M. L. Sampoli[b], A. Sestini[c]

[a]*Department of Mathematics and Computer Science, University of Parma, Parco Area delle Scienze, 53/A, Parma, Italy*
[b]*Department of Information Engineering and Mathematics, University of Siena, Via Roma 56, Siena, Italy*
[c]*Department of Mathematics and Computer Science, University of Florence, Viale Morgagni 67, Firenze, Italy*

Abstract

Isogeometric approach applied to Boundary Element Methods is an emerging research area (see e.g. [33]). In this context, the aim of the present contribution is that of investigating, from a numerical point of view, the Symmetric Galerkin Boundary Element Method (SGBEM) devoted to the solution of 2D boundary value problems for the Laplace equation, where the boundary and the unknowns on it are both represented by B-splines ([9]). We mainly compare this approach, which we call IGA-SGBEM, with a curvilinear SGBEM ([2]), which operates on any boundary given by explicit parametric representation and where the approximate solution is obtained using Lagrangian basis. Both techniques are further compared with a standard (conventional) SGBEM approach ([1]), where the boundary of the assigned problem is approximated by linear elements and the numerical solution is expressed in terms of Lagrangian basis. Several examples will be presented and discussed, underlying benefits and drawbacks of all the above-mentioned approaches.

Keywords: Isogeometric Analysis, B-splines, Symmetric Galerkin Boundary Element Method

1. Introduction

Boundary Element Methods (BEMs) have become an important technique for solving linear elliptic partial differential equations (PDEs) appearing in many relevant physical and engineering applications (e.g. potential, acoustics, elastostatics, etc.; see [23, 35, 40]). By means of the fundamental solution of the considered differential operator, a large class of both exterior and interior elliptic Boundary Value Problems (BVPs) can be formulated as a linear integral equation on the boundary of the given domain. The numerical analysis of these methods for 2D and 3D problems is now well studied ([1, 2, 3, 12, 23]). The BEM can offer substantial computational advantages over other approximation techniques, such as finite elements (FEM) or finite differences (FDM). Moreover, in some applications, the physically relevant information is not the solution inside the domain but rather its trace or its normal derivative on the domain boundary: these latter can be obtained directly from the numerical solution of Boundary Integral Equations (BIEs), whereas boundary values recovered from FEM solutions are not so accurate. However, in order to achieve an efficient numerical implementation of general validity, a number of issues have to be dealt with special attention. One of the most important, for the practical application of the BEM analysis, is the evaluation of singular integrals over boundary elements. It is only in these last decades that engineers and applied mathematicians have started employing finite part integrals to formulate several 2D and 3D BVPs, particularly in the area of applied mechanics, as singular and hypersingular BIEs in the so-called symmetric formulations ([23, 35]). Symmetric Galerkin Boundary Element

*Corresponding Author
Email addresses: alessandra.aimi@unipr.it (A. Aimi), mauro.diligenti@unipr.it (M. Diligenti), marialucia.sampoli@unisi.it (M. L. Sampoli), alessandra.sestini@unifi.it (A. Sestini)

Method (SGBEM) - see [7, 38] and references therein for rather complete surveys - is nowadays recognized as a valid alternative BEM technique for the solution of boundary value problems, yielding final symmetric discretization matrices which are suitable for the coupling with FEM ([42, 15]). Since its origins ([34]), a large amount of literature results has been produced for what concerns stability and convergence properties of the method related to smooth or piecewise smooth boundaries and to piecewise polynomial systems for the approximation of the BIE solution (see e.g. [40, 41, 31, 6, 30, 37]); further, great effort has been devoted to the development of efficient schemes for the double integration of weakly singular, Cauchy singular and hypersingular integrals over boundary elements ([2, 7, 22, 20]).

On the other side, isogeometric analysis (IGA) is a new method for the numerical treatment of problems governed by PDEs. In its first formulation introduced in the literature ([21]), the aim was to overcome some difficulties arising in FEMs, proposing a viable alternative to standard, polynomial-based, finite element analysis. Actually, the key issue in IGA is to retain the description of the domain where the PDE is defined as it is given by a Computer Aided Design (CAD) system (i.e., in terms of B-splines or their rational generalization, NURBS) instead of approximating it by a triangular/polygonal mesh. Note that the most domains of interest in engineering problems are exactly described in terms of B-splines or NURBS. The term *isogeometric* is due to the fact that the solution space for dependent variables is represented in terms of the same functions which describe the geometry of the domain. Thus, the isogeometric approach ensures an exact description of the domain at any level, no matter how coarse is the discretization of the problem. In addition, the mesh refinement is highly simplified because it can be obtained by standard *knot-insertion* and/or *degree-elevation* procedures ([18]), retaining the exact geometry of the original domain during the process and eliminating the need to communicate with the CAD system, once the initial mesh is constructed. In addition, the easier manipulation of smooth elements provides an efficient tool particularly well suited for high order equations. The above mentioned facts motivate the wide interest received by this new paradigm since the seminal paper [21] (see for example [26, 36, 39] and references quoted therein).

Very recently, literature on IGA has started dealing with applications involving BEMs (see e.g. [19, 28, 29, 33]), even if the germinal idea was pushed forward in [10, 11]. This new approach has been mostly compared with standard versions of the BEMs, based on a piecewise polygonal approximation of the boundary of the problem domain, obtaining, with no doubt, a remarkable superiority.

In this framework, we investigate, from a numerical point of view, the so-called IGA-SGBEM, i.e. the SGBEM devoted to the solution of 2D BVPs for the Laplace equation (but the analysis could be extended considering other operators), where B-splines are used to approximate the boundary geometry as well as the unknown potential and flux fields on it.

In order to combine IGA and SGBEM, we choose to work with B–spline basis, since it is a fundamental tool for dealing with polynomial spline spaces in the context of CAD and automatic manufacturing, where spline functions expressed in the B–spline basis (B–form) are the standard for free–form design ([18]). Furthermore, B-splines are also profitably used in several other fields, for example in multiresolution analysis or in collocation methods (see e.g. [25, 27]) and, as above mentioned, they are also the standard basis adopted in the recent context of IGA-FEM ([17]). The reason of this wide success depends on several aspects, surely because splines in B–form can be easily stored, evaluated and algebraically manipulated. Another important reason is that they have general features, very attractive for applications, such as nonnegativity, partition of unity, compact support, and total positivity ([9, 13]).

In this paper, IGA-SGBEM approach will be compared with curvilinear SGBEM ([2]) - an improved version with respect to the existing conventional boundary element techniques - which operates on any boundary given by explicit parametric representation (hence, in particular, given by B-splines representation), and where the approximate solution is obtained using Lagrangian basis. Both the above mentioned methods will be further compared with a standard (conventional) SGBEM approach ([1]), where the boundary of the assigned problem is approximated by linear elements and the numerical solution is expressed in terms of Lagrangian basis. Singular integrals required by SGBEMs are efficiently evaluated by suitable quadrature formulas with a very low number of quadrature nodes related to user assigned accuracy ([1, 2]). Several examples will be presented and discussed, underlying benefits and drawbacks of all the above mentioned techniques.

2. Model problem and its boundary integral formulation

Let $\Omega \subset \mathbb{R}^2$ be a bounded, simply connected, open domain with a (piecewise) smooth boundary $\Gamma := \partial\Omega = \{\mathbf{x} = (x_1, x_2) \in \mathbb{R}^2 | \mathbf{x} = \mathbf{C}(t),\ t \in [a, b]\}$, given by parametric representation on the interval $[a, b]$. Let us further suppose

that $\Gamma = \bar{\Gamma}_1 \cup \bar{\Gamma}_2$, where Γ_1 and Γ_2 are open disjoint subset of Γ and $meas\,(\Gamma_1) > 0$. As model problem, we consider a mixed BVP for the Laplace equation:

given $u^* \in H^{1/2}(\Gamma_1)$ *and* $q^* \in H^{-1/2}(\Gamma_2)$*, find* $u \in H^1(\Omega)$ *such that*

$$\begin{cases} \Delta u = 0 & \text{in } \Omega\,, \\ u = u^* & \text{on } \Gamma_1\,, \\ \frac{\partial u}{\partial \mathbf{n}} = q^* & \text{on } \Gamma_2\,, \end{cases} \tag{1}$$

where $\frac{\partial}{\partial \mathbf{n}}$ denotes the derivative with respect to the outer normal $\mathbf{n}$ to Γ. The definition of Sobolev spaces is as usual (see [24]).

As it is well known ([3, 16, 40]), from problem (1) the following identities for u and q on Γ can be derived:

$$\frac{1}{2}\begin{bmatrix} u \\ q \end{bmatrix} = \begin{bmatrix} -K & V \\ -D & K' \end{bmatrix}\begin{bmatrix} u \\ q \end{bmatrix}, \qquad \mathbf{x} \in \Gamma\,, \tag{2}$$

where

$$Vq(\mathbf{x}) := \int_\Gamma U(\mathbf{x},\mathbf{y})\, q(\mathbf{y}) \mathrm{d}\gamma_\mathbf{y}\,, \qquad Ku(\mathbf{x}) := \int_\Gamma \frac{\partial U}{\partial \mathbf{n}_\mathbf{y}}(\mathbf{x},\mathbf{y})\, u(\mathbf{y}) \mathrm{d}\gamma_\mathbf{y}$$

$$K'q(\mathbf{x}) := \int_\Gamma \frac{\partial U}{\partial \mathbf{n}_\mathbf{x}}(\mathbf{x},\mathbf{y})\, q(\mathbf{y}) \mathrm{d}\gamma_\mathbf{y}\,, \quad Du(\mathbf{x}) := \int_\Gamma \frac{\partial^2 U}{\partial \mathbf{n}_\mathbf{x} \partial \mathbf{n}_\mathbf{y}}(\mathbf{x},\mathbf{y})\, u(\mathbf{y}) \mathrm{d}\gamma_\mathbf{y}\,,$$

and

$$U(\mathbf{x},\mathbf{y}) := -\frac{1}{2\pi} \ln \|\mathbf{y}-\mathbf{x}\|_2\,,$$

is the fundamental solution of the 2D Laplace operator. Note that K and K' are defined by Cauchy singular integrals when Γ is a piecewise smooth boundary [1], while D is defined by a hypersingular finite part integral in the sense of Hadamard, i.e. it is understood to be the finite part of an asymptotic expansion ([32, 40]).

Under the above assumptions, the following properties are well known ([16, 32, 40]): the operators

$$\begin{aligned} &V : H^{-1/2+\sigma}(\Gamma) \to H^{1/2+\sigma}(\Gamma)\,, \qquad &&K : H^{1/2+\sigma}(\Gamma) \to H^{1/2+\sigma}(\Gamma)\,, \\ &K' : H^{-1/2+\sigma}(\Gamma) \to H^{-1/2+\sigma}(\Gamma)\,, \qquad &&D : H^{1/2+\sigma}(\Gamma) \to H^{-1/2+\sigma}(\Gamma)\,, \end{aligned} \tag{3}$$

are continuous for $\sigma \in (-\frac{1}{2}, \frac{1}{2})$. For $\sigma = 0$ the operator K' is the adjoint of K with respect to the natural duality $< \cdot, \cdot >$ between $H^{1/2}(\Gamma)$ and its dual $H^{-1/2}(\Gamma)$, which for sufficiently smooth functions coincides with the usual scalar product in $L^2(\Gamma)$.

The strong system of two BIEs (2) is, of course, overdetermined (see e.g. [7, 40]), hence it can be reformulated without redundancy, following an approach similar to the one rigorously developed in [4]. Therefore, by imposing the first equation only on Γ_1 and the second one only on Γ_2, and inserting the boundary data given in (1), we obtain a system of two BIEs of the first kind for the unknowns q on Γ_1 and u on Γ_2, of the form

$$\begin{bmatrix} V_{11} & -K_{12} \\ -K'_{21} & D_{22} \end{bmatrix}\begin{bmatrix} q \\ u \end{bmatrix} = \begin{bmatrix} -V_{12} & \frac{1}{2}I + K_{11} \\ -\frac{1}{2}I + K'_{22} & -D_{21} \end{bmatrix}\begin{bmatrix} q^* \\ u^* \end{bmatrix}, \tag{4}$$

where the boundary integral operators subscripts $j\,k$ mean evaluation over Γ_j and integration over Γ_k. Note that an alternative non redundant system of two BIEs of the second kind could be obtained considering the first equation only on Γ_2 and the second one only on Γ_1. However this latter approach does not lead to symmetric final discretization matrices.

System (4) will be solved in a weak sense (see [3, 40]). The weak formulation starts from identity (2): finding the weak solution $u \in H^1(\Omega)$ of BVP (1) is indeed equivalent to find the weak solution $[u,\, q] \in H^{1/2}(\Gamma) \times H^{-1/2}(\Gamma)$ of system (2) such that $u|_{\Gamma_1} = u^*$ and $q|_{\Gamma_2} = q^*$.

[1] In the case of a smooth boundary, the operators K and K' are only weakly singular ([5], Section 7).

After having recovered the missing Cauchy data by solving, with obvious meaning of notation, the weak symmetric ([7]) problem:

$$< \begin{bmatrix} V_{11} & -K_{12} \\ -K'_{21} & D_{22} \end{bmatrix} \begin{bmatrix} q \\ u \end{bmatrix}, \begin{bmatrix} p \\ v \end{bmatrix} >=< \begin{bmatrix} f_1 \\ f_2 \end{bmatrix}, \begin{bmatrix} p \\ v \end{bmatrix} >, \qquad \forall\, [p, v] \in H^{-1/2}(\Gamma_1) \times H_0^{1/2}(\Gamma_2)\,, \tag{5}$$

one can use the representation formula

$$u(\mathbf{x}) = \int_\Gamma U(\mathbf{x}, \mathbf{y})\, q(\mathbf{y}) \mathrm{d}\gamma_\mathbf{y} - \int_\Gamma \frac{\partial U}{\partial \mathbf{n}_\mathbf{y}}(\mathbf{x}, \mathbf{y})\, u(\mathbf{y}) \mathrm{d}\gamma_\mathbf{y}\,, \qquad \mathbf{x} \in \Omega\,,$$

to obtain the solution at any point of the domain.

Let us remember the advantages of using the symmetric boundary integral problem (4) for a mixed BVP: the unknowns on the boundary are directly those of the differential problem instead of density functions typical of indirect formulations ([14]); the linear system coming from the discretization of (5), due to the involved integral operators properties, presents a symmetric matrix and this, of course, is extremely important for what concerns saving computational time in matrix generation and memory in matrix storage.

Remark. If we have to deal with a Dirichlet BVP, i.e. $\Gamma \equiv \Gamma_1$, the systems (4) obviously reduces to the first equation alone, where the only unknown is $q(\mathbf{x})$. A similar boundary integral equation can be written for a Dirichlet problem exterior to an open arc in the plane (see e.g. [14]): in this case, the unknown is the jump of $q(\mathbf{x})$ across the arc Γ, i.e. $[q(\mathbf{x})]_\Gamma$.

3. Symmetric Galerkin Boundary Element Method

For the discretization phase, we consider a uniform partition of the parametrization interval $[a, b] = \bigcup_{\ell=1}^{n} I_\ell$, made up by n subintervals I_ℓ and governed by the decomposition parameter $h = length(I_\ell)$. This induces over Γ, using the parametric representation of the boundary, a mesh $\Gamma_h = \bigcup_{\ell=1}^{n} e_\ell$, constituted by curvilinear elements $e_\ell = \mathbf{C}(I_\ell)$.
In a similar way, a finite dimensional subspace of piecewise polynomial functions can then be lifted on the boundary, starting from the introduced partition of $[a, b]$.
In the IGA-SGBEM the very same B-spline basis used to represent the boundary Γ is used also as a basis for the functional approximation space; in the curvilinear SGBEM, the boundary can be given by any explicitly defined parametric representation (and therefore also by B-spline representation), but the approximation space is spanned by a Lagrangian basis defined over the decomposition of $[a, b]$.
At last, in the standard SGBEM, Γ is approximated by a polygonal boundary $\tilde{\Gamma}_h$, constituted by linear elements, each interpolating the endpoints of e_ℓ, $\ell = 1, \cdots, n$, and a local Lagrangian basis is lifted onto each straight element of $\tilde{\Gamma}_h$ from the reference element $[0, 1]$.

In any case, denoting with $\{\phi_i\}$ the basis of the functional approximation space where we will search the unknowns by means of Galerkin criteria, the elements of the final discretization linear system matrix will be double integrals of the form

$$\int_{\Gamma_h} \phi_j(\mathbf{x}) \int_{\Gamma_h} \mathcal{K}(\mathbf{x}, \mathbf{y}) \phi_i(\mathbf{y})\, d\gamma_\mathbf{y} d\gamma_\mathbf{x}\,, \tag{6}$$

(substituting Γ_h with $\tilde{\Gamma}_h$ in the case of standard SGBEM), where $\mathcal{K}$ denotes one of the kernels of the integral operators (3) and therefore it can be weakly singular, singular or hypersingular. Consequently, the inner integral in (6) has to be defined as generalized, Cauchy principal value or Hadamard finite part, respectively.
Then, using suitable numerical integration schemes to face all these types of singularities (see [1, 2]), one can write down the linear, symmetric, non singular system of equations

$$\begin{bmatrix} R_{11} & R_{12} \\ R_{21} & R_{22} \end{bmatrix} \begin{bmatrix} q_h \\ u_h \end{bmatrix} = \begin{bmatrix} b_1 \\ b_2 \end{bmatrix}, \tag{7}$$

where the vector unknowns q_h, u_h collect the coefficients with respect to the selected basis, which allow to finally obtain an approximate solution of the integral problem.

In the remaining part of the Section, we recall the definition of B-spline basis used in IGA-SGBEM approach, because it could be not necessarily known to people in the numerical simulation community. On the opposite, we do not recall the definition of the Lagrangian basis used below to compare IGA-SGBEM with curvilinear and standard SGBEMs, because it's more basic (anyway the interested reader can refer to [8]).

Given a partition $\Delta := \{a = t_0 < \cdots < t_n = b\}$ of an interval $[a, b]$, a general polynomial spline space S of order k on such partition is composed by piecewise polynomial functions of degree $k-1$ which are required to have an assigned regularity C^{k-1-m_i} at the breakpoints $t_i, i = 1, \ldots, n-1$, with m_i denoting an integer between 1 and k [2]. For example when all the m_i are fixed equal to 1 or to $k-1$ or to k, respectively S is a subset of $C^{k-2}[a, b]$, it is included in $C[a, b]$ or it is just a subset of $L^2(a, b)$. It is quite easy to verify that the dimension of such space is $dim(S) = k + \sum_{i=1}^{n-1} m_i$. The easiest way to define in S a B-spline basis $B_{i,k}(t), i = 0, \ldots, N$, with $N+1 = dim(S)$, is based on the usage of a recursion formula and can be described through two easy steps ([9]). The first step consists in associating to S an *extended knot vector* $T = \{\tau_0, \cdots, \tau_{N+k}\}$ whose elements constitute a non decreasing sequence of abscissas, where $\{\tau_{k-1}, \cdots, \tau_{N+1}\}$ are the *internal knots* with $\tau_{k-1} = t_0$, $\tau_{N+1} = t_n$ and $\{\tau_k, \cdots, \tau_N\} = \{t_1, \cdots, t_1, \cdots, t_{n-1}, \cdots, t_{n-1}\}$, where each t_i has m_i occurrences and it is said *multiple* if $m_i > 1$. The remaining knots in T, $\{\tau_0, \cdots, \tau_{k-2}\}$ and $\{\tau_{N+2}, \cdots, \tau_{N+k}\}$ form two sets of $(k-1)$ knots called *auxiliary left* and *right knots* which are only required to verify the following inequalities, $\tau_0 \leq \cdots \leq \tau_{k-2} \leq \tau_{k-1} = a$ and $b = \tau_{N+1} \leq \tau_{N+2} \leq \cdots \leq \tau_{N+k}$. Note that, in the numerical simulations, we will always use the standard assumption of selecting an *open* extended knot vector, that is $\tau_0 = \cdots = \tau_{k-2} = \tau_{k-1} = a$ and $b = \tau_{N+1} = \tau_{N+2} = \cdots = \tau_{N+k}$.
In the second step, the basis is defined by using the following recursion ([9]):

$$B_{i,1}(t) := \begin{cases} 1, & \text{if } \tau_i \leq t < \tau_{i+1}, \\ 0, & \text{otherwise.} \end{cases}$$

$$B_{i,j}(t) := \omega_{i,j}(t)\, B_{i,j-1}(t) + (1 - \omega_{i+1,j}(t))\, B_{i+1,j-1}(t), \quad 1 < j \leq k,$$

with $\omega_{i,j}(t) := \begin{cases} \frac{t-\tau_i}{\tau_{i+j-1}-\tau_i} & \text{if } \tau_i < \tau_{i+j-1}, \\ 0 & \text{otherwise.} \end{cases}$

Note that from the above recursive definition it is easy to verify the nonnegativity of B-splines and that the support of $B_{i,k}$ is the subinterval $[\tau_i, \tau_{i+k}]$. The partition of unity property can also be easily proved by induction on the order.

As an example, in Figure 1, the plots of all B-splines spanning two different quadratic spline spaces S_1 and S_2, respectively of dimension $N + 1 = 13$ and $N + 1 = 15$, can be seen. Such spaces share the same partition $\{t_i = i, i = 0, \ldots, 9\}$ of the interval $[0, 9]$ but their extended knot vectors are T_1 on the left and T_2 on the right, with

$$\begin{aligned} T_1 &= [0, 0, 0, 1, 1, 2, 3, 4, 5, 6, 7, 8, 8, 9, 9, 9], \\ T_2 &= [0, 0, 0, 1, 1, 1, 2, 3, 4, 5, 6, 7, 8, 8, 8, 9, 9, 9]. \end{aligned} \tag{8}$$

4. Numerical results

From now on, we will indicate curvilinear and standard SGBEMs with C-SGBEM and S-SGBEM, respectively.

Example 1.

In this example we consider a potential problem interior to the domain shown in Figure 2, which has three sharp corners and is similar to that one constructed by means of NURBS in [33]. The boundary of the domain is in our case described by a closed parametric piecewise quadratic curve, $\mathbf{C}(t)$, $t \in [0, 9]$, with integer uniform breakpoints $t_i = i$, $i = 0, \ldots, 9$. Such curve can be represented in B-form, that is as a linear combination of the quadratic B-splines

[2] When $m_i = k$ this means that the function has a finite jump at $t = t_i$.

(see Figure 1, left) associated to the extended knot vector T_1 given in (8) and control points $\mathbf{Q}_i$, $i = 0\ldots, 12$, whose coordinates are given in the following matrix:

$$Q = \begin{bmatrix} 0 & 0.5 & 1 & 1 & 0 & -1 & -1 & -1 & 0 & 1 & 1 & 0.5 & 0 \\ 0 & 0.125 & 0.25 & 1 & 1 & 1 & 0 & -1 & -1 & -1 & -0.25 & -0.125 & 0 \end{bmatrix}.$$

Note that the curve is closed because $\mathbf{Q}_0 = \mathbf{Q}_{12}$ but its regularity at the initial/final joint point is only C^0 because T_1 is an open extended knot vector. Moreover, considering the double multiplicity of the breakpoints t_1 and t_8 specified in T_1, it turns out that $\mathbf{C}(t) \in C^0[0, 9] \cap C^1[1, 8]$. In this way, the geometry of the domain boundary can be exactly described.

The differential problem is equipped with Dirichlet boundary condition $u^*(\mathbf{x}) = -(x_1 + x_2)$; the solution of the related boundary integral equation is explicitly known, it reads $q(\mathbf{x}) = q(\mathbf{C}(t)) = (C_1'(t) - C_2'(t))/\|\mathbf{C}'(t)\|_2$ and has $L^2(0, 9)$ regularity. In particular it presents a jump discontinuity at $t = t_1$, $t = t_8$ and at $t = t_0$ ($t = t_9$), while it is only C^0 in the remaining breakpoints.

As a first choice, we do not care about the low regularity of the solution and we work in the space used to describe the boundary which is spanned by the quadratic B-splines associated to T_1 and is a subset of $C^0[0, 9] \cap C^1[1, 8]$. Then we successively extend the space by inserting a new simple knot at the midpoint between any two successive breakpoints (this corresponds to halving the mesh step h, since uniform distributions of the breakpoints are always assumed).

In Table 1, the obtained results are shown: for each considered h, the corresponding total number of degrees of freedom (DoF), the spectral condition number of the matrix in (7), and the relative error

$$E =: \|q - q_h\|_{L^2}/\|q\|_{L^2}\,, \tag{9}$$

are given.

Figure 3 confirms that the numerical solution obtained with $h = 1/8$ mainly agrees with the analytical solution. As expected, the jumps are smoothly approximated; small oscillations occur in the neighborhood of the jumps, especially around $t = 1$.

In order to adequate the quadratic spline space to the regularity of the analytical solution, we have then performed a similar set of experiments starting now from the extended knot vector T_2, given in (8). The associated $L^2(0, 9) \cap C^1[1, 8]$ quadratic B-spline basis is shown in Figure 1, right.

In Table 2, we show the comparison between the results obtained successively refining the parameter h for the $L^2(0, 9) \cap C^1[1, 8]$ quadratic B-splines in IGA-SGBEM and the $L^2(0, 9) \cap C^0[1, 8]$ quadratic Lagrangian basis in C-SGBEM. In particular, for both approaches, we present the total number of degrees of freedom (DoF), the spectral condition number of the associated linear system matrix and the relative error (9).

Final errors are better than the corresponding ones shown in Table 1, even if we note an error stagnation, for either IGA-SGBEM and C-SGBEM. This is due to the difficulty of recovering the analytical solution near the jumps, in particular on the side of the jumps where the exact solution is constant, even if, anyway, the approximation sensibly improves elsewhere, as it is shown in Fig. 4. Actually, for this kind of solutions, as well as for solutions exhibiting sharp layers, the use of generalized exponential spline spaces could be more suitable ([26]) and it is planned as future work.

Example 2.

In the second example we consider a potential problem interior to the domain shown in Figure 5, see [28]. Such domain has a smooth boundary that can be described by a closed parametric piecewise cubic curve, $\mathbf{C}(t)$, $t \in [0, 1]$, with uniform breakpoints and mesh step $h = 1/8$. This curve can be represented in B-form with extended knot vector

$$T_3 = [0,\ 0,\ 0,\ 0,\ 0.125,\ 0.25,\ 0.375,\ 0.5, 0.625,\ 0.75,\ 0.875,\ 1,\ 1,\ 1,\ 1]$$

and control points $\mathbf{Q}_i$, $i = 0\ldots, 10$, whose coordinates are collected in the following matrix:

$$Q = \begin{bmatrix} -16 & -22 & -1 & 2 & 29 & 1 & 32 & 12 & 4 & -10 & -16 \\ 11.5 & 6.5 & 2 & -15 & -8 & -4 & 17 & 19 & 1 & 16.5 & 11.5 \end{bmatrix}.$$

The differential problem is equipped with Dirichlet boundary condition $u^*(\mathbf{x}) = -(x_1 + x_2)$; as in the previous example, the solution $q(\mathbf{x})$, $\mathbf{x} = \mathbf{C}(t)$, of the related boundary integral equation is explicitly known, but now, as function of t, it is C^1 regular on $[0, 1]$.

For this example, we first present a comparison between the results obtained working in nested C^2 spline spaces of increasing degree ≥ 3, spanned by the B-spline basis (IGA-SGBEM), and working with larger C^0 spline spaces of corresponding degree spanned by the Lagrangian basis (C-SGBEM). Note that the boundary curve can be exactly expressed in all the considered spaces and its representation can be obtained combining a *degree elevation* with a *knot insertion* procedures (see e.g. [18]).

The recalled basis functions regularity, which defines the type of norms that can be used to estimate the approximation error ([31]), allows us to compare the different approaches considering the relative error E defined in (9), as done in the previous example. Results are presented in Table 3 and the errors are then plotted in Figure 6 with respect to DoF.

Then, in Tables 4 and 5, results obtained considering two successive halving of the mesh size h are reported. The corresponding error behaviors are shown in Figures 7 and 8, respectively: the rate of convergence of both methods are almost equal, although, using IGA-SGBEM we can achieve the same error with fewer DoFs w.r.t. C-SGBEM. This is due to the fact that in the so-called *p-version* of the Galerkin BEM ([37, 30]), where the accuracy is reached fixing the mesh and elevating the degree of the piecewise polynomial basis, the error mainly depends on this degree (order).

Further, note that in these simulations the conditioning of B-splines systems are worse than the corresponding Lagrangian ones. Anyway, the remarkable shape reproduction capability of our scheme is underlined in Figure 9 which shows the approximate solution obtained with $h = 1/16$ and the B-spline basis of degree 9 together with the analytical solution.

Finally, in order to put in evidence possible benefits of our approach, we fix now the degree of the piecewise polynomial spaces equal to 3 and compare the results obtained using C^2 B-spline basis in IGA-SGBEM and C^0 Lagrangian basis in C-SGBEM. The comparison is first done in Table 6, with respect to h, where results obtained using C^1 B-spline basis in IGA-SGBEM are also given. We note that the errors with the IGA-SGBEM approach are slightly worse, but the degrees of freedom are remarkably lower.

The benefits of our approach can be better observed looking at Table 7, where indeed the comparison is done with respect to DoF. Such a comparison can be achieved by selecting, for a given value of DoF, a suitable mesh size h. To complete this benchmark, on the right of Table 7, for the same DoF, relative errors obtained using L^2 cubic Lagrangian basis on piecewise linear approximation $\tilde{\Gamma}_h$ of the boundary Γ are reported. All the errors of these last Table are plotted in Figure 10 with respect to DoF. This graphic reveals the inferiority of the standard SGBEM approach with respect to IGA and curvilinear SGBEMs, due to the introduced approximation of the boundary.

Example 3.

Since one of the major strengths of BEM approach (with respect to FEM) is its ability of easily treating domains with holes, let us now consider the two trimmed domains depicted in Figure 11. For the domain on the left (A), the two boundary curves are represented by cubic B-splines with extended knot vector

$$T_4 = [0, 0, 0, 0, 1/6, 2/6, 3/6, 4/6, 5/6, 1, 1, 1, 1],$$

while the curves defining the domain on the right (B), are quartic B-splines with extended knot vector

$$T_5 = [0, 0, 0, 0, 0, 1/5, 2/5, 3/5, 4/5, 1, 1, 1, 1, 1].$$

The coordinates of the control points associated to the external and internal boundary curves are collected in the following matrices:

$$Q_{\text{est}_\text{A}} = \begin{bmatrix} 1 & 1 & 0 & -1 & -1 & -1 & 0 & 1 & 1 \\ 0 & 1 & 1 & 1 & 0 & -1 & -1 & -1 & 0 \end{bmatrix},$$

$$Q_{\text{int}_\text{A}} = \begin{bmatrix} 0.25 & 0.25 & -0.25 & -0.75 & -0.75 & -0.75 & -0.25 & 0.25 & 0.25 \\ 0.25 & -0.25 & -0.25 & -0.25 & 0.25 & 0.75 & 0.75 & 0.75 & 0.25 \end{bmatrix}.$$

$$Q_{\text{est}_\text{B}} = \begin{bmatrix} 1 & 1 & 0 & -1 & -1 & -1 & 0 & 1 & 1 \\ 0 & 1 & 1 & 1 & 0 & -1 & -1 & -1 & 0 \end{bmatrix},$$

$$Q_{\text{int}_B} = \begin{bmatrix} -0.25 & -0.25 & -0.5 & -0.75 & -0.75 & -0.75 & -0.5 & -0.25 & -0.25 \\ 0.5 & 0.25 & 0.25 & 0.25 & 0.5 & 0.75 & 0.75 & 0.75 & 0.5 \end{bmatrix}.$$

For both domains a mixed BVP is considered, where a Dirichlet condition $u^* = 1$ is assigned on the interior boundary, while a Neumann condition $q^* = 0$ is prescribed on the exterior boundary. This configuration can model a stationary heat conduction problem, where a constant temperature on the inner wall and a zero heat flux on the outer wall are given.

Focusing on domain A, we have tested our IGA-SGBEM approach just using the cubic spline space used to define the boundary curves ($h = 1/6$). The resulting linear system is of order 16 and the approach produces an approximate solution with an absolute error E_M in maximum norm equal to $1.9451\,10^{-5}$ for what concerns the recovered flux q and equal to $2.1153\,10^{-5}$ for what concerns the recovered potential u. If we use cubic C-SGBEM, instead, we have to solve a liner system of order 36 to reproduce the same error order.

Regarding domain B, we have again tested our scheme just considering the quartic spline space used to describe the boundaries ($h = 1/5$). Again we end up with a linear system of order 16, which produces an approximate solution with an absolute error E_M in maximum norm equal to $3.7748\,10^{-5}$ for what concerns the recovered flux q and equal to $3.7301\,10^{-5}$ for what concerns the recovered potential u. If we use quartic C-SGBEM, instead, we have to solve a liner system of order 40 to reproduce the same error order.

Remark. Here, we have chosen to evaluate the absolute error E_M in maximum norm instead of (9) since the considered mixed boundary conditions allow the BVP to have the constant solution $u = 1$. The obtained errors are due to the approximation of weakly singular, singular and hypersingular double integrals by means of the already mentioned quadrature formulas ([2]).

Example 4.

Let us conclude this Section, considering a Dirichlet BVP for the Laplace equation exterior to the arc of parabola $\Gamma = \{\mathbf{x} = (x_1, x_2) | \, x_1 = t, \; x_2 = 1 - t^2, \; t \in [a, b] = [-1, 1]\}$, representable by means of quadratic B-splines related to the extended knot vector

$$T_6 = \begin{bmatrix} -1 & -1 & -1 & 1 & 1 & 1 \end{bmatrix}$$

and to the control points $\mathbf{Q}_i$, $i = 0, \cdots, 2$, whose coordinates are collected in the following matrix:

$$Q = \begin{bmatrix} -1 & 0 & 1 \\ 0 & 2 & 0 \end{bmatrix}.$$

The considered differential problem can model the electrostatic problem of finding the electric potential around a condenser, whose two faces are so near one another to be considered as overlapped, knowing the electric potential only on the condenser. Here the Dirichlet datum is given in such a way that the solution of the related boundary integral equation is explicitly known and reads $[q(\mathbf{x})]_\Gamma = \sqrt{1 + 4x_1^2}$.

The comparison reported in Table 8, for different values of the parameter h, which uniformly decomposes the parameter interval $[-1, 1]$, involves C^1 quadratic B-spline basis for IGA-SGBEM, C^0 quadratic Lagrangian basis for C-SGBEM and L^2 quadratic Lagrangian basis on piecewise linear approximation $\tilde{\Gamma}_h$ of Γ for S-SGBEM. Together with DoF and spectral condition numbers of the associated matrices, we show the absolute errors E_M in maximum norm. These errors are visualized in Figure 12 with respect to DoF.

At last, for this example, in Table 9 we show a comparison between Galerkin IGA-BEM described in this paper and collocation IGA-BEM, where collocation is done at the Greville abscissae as in [33]. It turns out that, for a fixed discretization parameter h, the Galerkin technique is more accurate than the collocation one, while the matrix condition number of the latter is better, even if the symmetry property useful in the coupling with FEM ([42, 15]) is lost. Both techniques, as shown in this Table, satisfy the estimates given in [31] for what concerns the decay of Galerkin error E_M, which, for smooth boundaries and sufficiently regular data, behaves as $O(h^k)$, being k the order of the fixed B-spline basis.

5. Conclusions

In this work we studied from a numerical point of view an Isogeometric Symmetric Galerkin Boundary Element Method, which we called IGA-SGBEM, dealing with the reference 2D Laplace problem, on domains having different

shapes. In particular our aim was to compare the performances of such approach not only with those of standard SGBEM (where the boundary of the domain is approximated by polygonal lines), but also with those of a more advanced SGBEM, namely curvilinear SGBEM, which is capable of retaining the exact boundary.

The potential strength and superiority of the presented approach has been confirmed by all the numerical tests, where smooth and non smooth interior domains as well as domains with holes or unbounded domains exterior to an open arc have been considered. The only drawback of IGA-SGBEM is, in few cases involving very long boundary elements, the worse conditioning of the discretization linear system matrix, which is probably due to the larger support of B-splines with respect to that one of the Lagrangian basis functions.

In order to better exploit the potentiality of the isogeometric approach combined with SGBEM we plan, as a future work, to extend the analysis to non polynomial spline spaces, able to represent exactly complex shapes. This can be achieved by considering generalized B-splines ([26]). The extension of our approach to 3D problems would constitute a further challenge, where its major appeal with respect to classical IGA-FEM could be more evident.

Acknowledgements

This work has been partially supported by INdAM, through GNCS research projects.

References

[1] A. Aimi, M. Diligenti, G. Monegato, New numerical integration schemes for applications of Galekin BEM to 2D problems, Internat. J. Numer. Methods Engrg. **40**, 1977–1999, (1997).
[2] A. Aimi, M. Diligenti, G. Monegato, Numerical integration schemes for the BEM solution of hypersingular integral equations, Internat. J. Numer. Methods Engrg. **45**, 1807–1830, (1999).
[3] A. Aimi, M. Diligenti, Hypersingular kernel integration in 3D Galerkin boundary element method, J. Comput. Appl. Math. **138**, 51–72, (2002).
[4] H. Andra, E. Schnack, Integration of singular Galerkin-type boundary element integrals for 3D elasticity problems, Numer. Math. **76**, 143–165, (1997).
[5] K.E. Atkinson, The Numerical Solution of Integral Equations of the Second Kind, Cambridge University Press, (2009, digital printed version).
[6] I.Babuska, B.Q. Guo, E.P. Stephan, On the exponential convergence of the h-p version for Boundary Element Galerkin Methods on Polygons, *Math. Methods Appl. Sci.*, **12** 413-427, (1990).
[7] M. Bonnet, G. Maier, C. Polizzotto, Symmetric Galrkin boundary element methods, Appl. Mech. Rev. **51**(11), 669–704, (1998).
[8] C.A. Brebbia, J.C.F. Telles, L.C. Wrobel, Boundary element techniques: theory and applications in engineering, Springer-Verlag, New York, (1984).
[9] C. de Boor, A Practical Guide to Splines, Revised edition, Applied Mathematical Sciences 27, Springer-Verlag, New York, (2001).
[10] J.J.S.P. Cabral, L.C. Wrobel, C.A. Brebbia, A BEM formulation using B-splines: I-uniform blending functions, Eng. Anal. Boundary Elem. **7**(3), 136–144, (1990).
[11] J.J.S.P. Cabral, L.C. Wrobel, C.A. Brebbia, A BEM formulation using B-splines: II-multiple knots and non-uniform blending functions, Eng. Anal. Boundary Elem. **8**(1), 51–55, (1991).
[12] A. Carini, M. Diligenti, P. Maranesi, M. Zanella, Analytical integrations for two-dimensional elastic analysis by the symmetric Galerkin boundary element method, Comput. Mech. **23**, 308–323, (1999).
[13] J.M. Carnicer, J. M Pena, Total positivity and optimal bases. Total positivity and its applications (Jaca, 1994), Math. Appl. **359**, Kluwer Acad. Publ., Dordrecht, 133–155, (1996).
[14] G. Chen, J. Zhou, Boundary Element Methods, Computational Mathematics and Applications, Academic Press, London, (1992).
[15] M. Costabel, Symmetric Methods for the coupling of Finite Elements and Boundary elements, in: C.A. Brebbia, W.L. Wendland and G. Kuhn (eds.) **1**, Springer-Verlag, (1987).
[16] M. Costabel, Boundary integral operators on Lipschitz domains: elementary results, SIAM J. Math. Anal. **19** (3), 613–626, (1998).
[17] J. A. Cottrell, T. J. R. Hughes, Y. Bazilevs; Isogeometric Analysis: Toward Integration of CAD and FEA, John Wiley & Sons, (2009).
[18] G. Farin, J. Hoschek, M.-S. Kim (Eds.), *Handbook of Computer Aided Geometric Design*, Elesevier Amsterdam, (2002).
[19] M. Feischl, G. Gantner, D. Praetorius, A Posteriori Error Estimation for Adaptive Iga Boundary Element Methods, in: E. Oñate, J. Oliver and A. Huerta (Eds.) *Proceeding of ECCM V*, 2421–2432, (2014).
[20] S.M. Holzer, How to deal with hypersingular integrals in the symmetric BEM. Comm. Numer. Meth. Engng. **9**, 219–232, (1993).
[21] T.J.R. Hughes, J.A. Cottrell , Y. Bazilevs, Isogeometric analysis: CAD, finite elements, NURBS, exact geometry and mesh refinement, *Comput. Methods Appl. Mech. Engrg.* **194**, 4135–4195, (2005).
[22] J.H. Kane, C. Balakrishna, Symmetric Galerkin boundary formulations emplying curved element, Internat. J. Numer. Methods Engrg. **36**, 2157–2187, (1993).
[23] G. Krishnasamy,L.W. Schmerr, T.J. Rudolphi, F.J. Rizzo, Hypersingular boundary integral equations: some applications in acoustic and elastic wave scattering, Trans. ASME Ser. J. Appl. Mech. **57**, 404–414, (1990).
[24] J.L. Lions, E. Magenes, Non-homogeneous Boundary value Problems and Application I, Springer, Berlin, Heidelberg, NewYork, (1972).
[25] T. Lyche, K. Mørken, E. Quak, Theory and algorithms for nonuniform spline wavelets. Multivariate approximation and applications, Cambridge Univ. Press, Cambridge, 152–187, (2001).

[26] C. Manni, F. Pelosi, M. L. Sampoli, Generalized B-splines as a tool in Isogeometric Analysis, *Comput. Methods Appl. Mech. Engrg.* **200**, 867–881, (2011).
[27] F. Mazzia, A. Sestini, D. Trigiante, B-spline Linear Multistep Methods and their Continuous Extensions, Siam J. of Numer. Anal. **44**, No. 5, 1954–1973, (2006).
[28] C.G. Politis, A.I. Ginnis, P.D. Kaklis, K. Belibassakis, C. Feurer, An isogeometric BEM for exterior potential-flow problems in the plane, SIAM/ACM Joint Conference on Geometric and Physical Modeling, 349–354, (2009).
[29] C.G. Politis, A. Papagiannopoulos, K.A. Belibassakis, P.D. Kaklis, K.V. Kostas, A.I. Ginnis and T.P. Gerostathis, An Isogeometric BEM for Exterior Potential-Flow Problems around Lifting Bodies, in: E. Oñate, J. Oliver and A. Huerta (Eds.) *Proceeding of ECCM V*, 2433–2444, (2014).
[30] F.V. Postell, E.P. Stephan, On the h-,p- and h-p versions of the boundary element method- Numerical results, Comp. Methods Appl. Mech. Eng. **83**, 69–89, (1990).
[31] R. Rannacher, W.L. Wendland, On the order of pointwise convergence of some boundary element methods. Part I. Operators of negative and zero order, Math. Model. Numer. Anal. **19**(1), 65-88, (1985).
[32] C. Schwab, W.L. Wendland, Kernel properties and representations of boundary integral operators, Math. Nachr. **156**, 156–218, (1992).
[33] R.N. Simpson, S.P.A. Bordas, J. Trevelyan, T. Rabczuk, A two-dimensional Isogeometric Boundary Element Method for elastostatic analysis, Comput. Methods Appl. Mech. Engrg. **209-212**, 87–100, (2012).
[34] S. Sirtori, General stress analysis method by means of integral equations and boundary elements, Meccanica **14**, 21–218, (1979).
[35] S. Sirtori, G. Maier, G. Novati, S. Micoli, A Galerkin symmetric boundary element method in elasticity: formulation and implementation, Internat. J. Numer. Methods Engrg. **35**, 255–282, (1992).
[36] H. Speleers, C. Manni, F. Pelosi, M. L. Sampoli, Isogeometric analysis with Powell-Sabin splines for advection-diffusion-reaction problems, *Comput. Methods Appl. Mech. Engrg.* **221–222**, 132–148, (2012).
[37] E.P. Stephan, M. Suri, On the convergence of the p-version of the Boundary Element Galerkin Method, Math. Comp. **52**(185), 31-48, (1989).
[38] A. Sutradhar, G.H. Paulino, L.J. Gray, Symmetric Galerkin Boundary Element Method, Springer, (2008).
[39] A.-V. Vuong, C. Giannelli, B. Jüttler, B. Simeon, A hierarchical approach to adaptive local refinement in isogeometric analysis, *Comput. Methods Appl. Mech. Engrg.* **200**, 3554–3567, (2011).
[40] W.L. Wendland, On some mathematical aspects of boundary element methods for elliptic problems, in: *The Mathematics of Finite Elements and Applications V*, Academic Press, London, (1985).
[41] W.L. Wendland, Boundary Element Methods for Elliptic Problems , in A.H.Schatz, V.Thome and W.L.Wendland (Eds.), *Mathematical theory of Finite and Boundary Ekement Methods*, Birkhauser, 219-276, (1990).
[42] W.L. Wendland, Variational Methods for BEM, in: L.Morino, R.Piva (eds) *Boundary Integral Equation Methods -Theory and Applications*, Springer-Verlag, (1990).

h	DoF	cond.	E
1	13	$2.53\,10^{2}$	$3.32\,10^{-1}$
1/2	22	$3.05\,10^{2}$	$1.61\,10^{-1}$
1/4	40	$5.82\,10^{2}$	$1.08\,10^{-1}$
1/8	76	$1.23\,10^{3}$	$7.62\,10^{-2}$

Table 1: Example 1: results obtained by quadratic B-splines starting from extended knot vector T_1.

	IGA-SGBEM			C-SGBEM		
h	DoF	cond.	E	DoF	cond.	E
1	15	$4.23\,10^{2}$	$2.06\,10^{-1}$	21	$1.68\,10^{2}$	$4.56\,10^{-2}$
1/2	24	$3.55\,10^{2}$	$5.20\,10^{-2}$	39	$2.68\,10^{2}$	$1.84\,10^{-2}$
1/4	42	$5.68\,10^{2}$	$1.83\,10^{-2}$	75	$5.38\,10^{2}$	$2.35\,10^{-2}$
1/8	78	$1.21\,10^{3}$	$1.84\,10^{-2}$	147	$1.09\,10^{3}$	$3.34\,10^{-2}$

Table 2: Example 1: comparison between results obtained with quadratic $L^2(0,9)\cap C^1[1,8]$ B-splines/ $L^2(0,9)\cap C^0[1,8]$ Lagrangian basis, varying h.

$h = 1/8$	IGA-SGBEM			C-SGBEM		
degree	DoF	cond.	E	DoF	cond.	E
3	10	$6.61\,10^{2}$	$3.37\,10^{-1}$	24	$5.47\,10^{2}$	$4.69\,10^{-2}$
4	18	$4.07\,10^{3}$	$1.26\,10^{-1}$	32	$1.21\,10^{3}$	$3.43\,10^{-2}$
5	26	$1.89\,10^{4}$	$6.55\,10^{-2}$	40	$2.02\,10^{3}$	$2.34\,10^{-2}$
6	34	$9.19\,10^{4}$	$3.23\,10^{-2}$	48	$4.42\,10^{3}$	$1.56\,10^{-2}$
7	42	$4.40\,10^{5}$	$1.71\,10^{-2}$	56	$5.50\,10^{3}$	$1.17\,10^{-2}$
8	50	$2.08\,10^{6}$	$1.03\,10^{-2}$	64	$1.88\,10^{4}$	$8.51\,10^{-3}$
9	58	$9.84\,10^{6}$	$3.57\,10^{-3}$	72	$1.45\,10^{4}$	$3.26\,10^{-3}$

Table 3: Example 2: comparison between results obtained with IGA-SGBEM based on C^2 B-splines and C-SGBEM based on C^0 Lagrangian basis, for different degrees of the piecewise polynomial basis and $h = 1/8$.

$h = 1/16$	IGA-SGBEM			C-SGBEM		
degree	DoF	cond.	E	DoF	cond.	E
3	18	$1.18\,10^{3}$	$1.28\,10^{-1}$	48	$1.49\,10^{3}$	$1.85\,10^{-2}$
4	34	$7.78\,10^{3}$	$4.06\,10^{-2}$	64	$3.36\,10^{3}$	$1.13\,10^{-2}$
5	50	$3.72\,10^{4}$	$1.44\,10^{-2}$	80	$5.30\,10^{3}$	$6.32\,10^{-3}$
6	66	$1.90\,10^{5}$	$4.92\,10^{-3}$	96	$1.16\,10^{4}$	$2.52\,10^{-3}$
7	82	$9.69\,10^{5}$	$1.97\,10^{-3}$	112	$1.35\,10^{4}$	$1.10\,10^{-3}$
8	98	$4.98\,10^{6}$	$7.31\,10^{-4}$	128	$4.93\,10^{4}$	$4.31\,10^{-4}$
9	114	$2.51\,10^{7}$	$4.08\,10^{-4}$	144	$3.49\,10^{4}$	$3.74\,10^{-4}$

Table 4: Example 2: comparison between results obtained with IGA-SGBEM based on C^2 B-splines and C-SGBEM based on C^0 Lagrangian basis, for different degrees of the piecewise polynomial basis and $h = 1/16$.

$h = 1/32$	IGA-SGBEM			C-SGBEM		
degree	DoF	cond.	E	DoF	cond.	E
3	34	$2.44\,10^{3}$	$4.11\,10^{-2}$	96	$4.21\,10^{3}$	$5.38\,10^{-3}$
4	66	$2.21\,10^{4}$	$7.81\,10^{-3}$	128	$8.84\,10^{3}$	$1.52\,10^{-3}$
5	98	$1.13\,10^{5}$	$1.63\,10^{-3}$	160	$1.32\,10^{4}$	$2.74\,10^{-4}$
6	130	$5.90\,10^{5}$	$3.80\,10^{-4}$	192	$2.77\,10^{4}$	$1.60\,10^{-4}$
7	162	$3.08\,10^{6}$	$1.28\,10^{-4}$	224	$3.09\,10^{4}$	$9.40\,10^{-5}$
8	194	$1.59\,10^{7}$	$3.86\,10^{-5}$	256	$1.12\,10^{5}$	$3.23\,10^{-5}$
9	226	$8.08\,10^{7}$	$1.28\,10^{-5}$	288	$7.53\,10^{4}$	$6.36\,10^{-6}$

Table 5: Example 2: comparison between results obtained with IGA-SGBEM based on C^2 B-splines and C-SGBEM based on C^0 Lagrangian basis, for different degrees of the piecewise polynomial basis and $h = 1/32$.

	C^2 IGA-SGBEM			C^1 IGA-SGBEM			C^0 C-SGBEM		
h	DoF	cond.	E	DoF	cond.	E	DoF	cond.	E
1/8	10	$6.61\,10^{2}$	$3.37\,10^{-1}$	17	$1.29\,10^{3}$	$1.30\,10^{-1}$	24	$5.47\,10^{2}$	$4.69\,10^{-2}$
1/16	18	$1.18\,10^{3}$	$1.28\,10^{-1}$	25	$2.17\,10^{3}$	$6.23\,10^{-2}$	48	$1.49\,10^{3}$	$1.85\,10^{-2}$
1/32	34	$2.44\,10^{3}$	$4.11\,10^{-2}$	41	$3.99\,10^{3}$	$1.95\,10^{-2}$	96	$4.21\,10^{3}$	$5.38\,10^{-3}$
1/64	66	$7.48\,10^{3}$	$8.29\,10^{-3}$	73	$1.19\,10^{4}$	$2.63\,10^{-3}$	192	$1.10\,10^{4}$	$4.92\,10^{-4}$

Table 6: Example 2: comparison among results obtained with cubic C^2 B-splines (left), cubic C^1 B-splines (middle) and cubic C^0 Lagrangian basis (right).

	IGA-SGBEM			C-SGBEM			S-SGBEM		
DoF	h	cond.	E	h	cond.	E	h	cond.	E
24	1/22	$1.63\,10^{3}$	$9.53\,10^{-2}$	1/8	$5.47\,10^{2}$	$4.69\,10^{-2}$	1/6	$3.01\,10^{2}$	$6.54\,10^{-1}$
48	1/46	$4.25\,10^{3}$	$2.75\,10^{-2}$	1/16	$1.49\,10^{3}$	$1.85\,10^{-2}$	1/12	$1.26\,10^{3}$	$5.06\,10^{-1}$
96	1/94	$1.46\,10^{4}$	$3.70\,10^{-3}$	1/32	$4.21\,10^{3}$	$5.38\,10^{-3}$	1/24	$1.59\,10^{3}$	$1.41\,10^{-1}$
192	1/190	$4.57\,10^{4}$	$2.08\,10^{-4}$	1/64	$1.10\,10^{4}$	$4.92\,10^{-4}$	1/48	$5.29\,10^{3}$	$4.82\,10^{-2}$

Table 7: Example 2: comparison between results obtained with cubic C^2 B-splines (left), C^0 Lagrangian basis (middle), L^2 Lagrangian basis on $\tilde{\Gamma}_h$ (right), for different values of DoF.

	IGA-SGBEM			C-SGBEM			S-SGBEM		
h	DoF	cond.	E_M	DoF	cond.	E_M	DoF	cond	E_M
1/10	22	$1.87\,10^{2}$	$2.11\,10^{-5}$	41	$2.33\,10^{2}$	$4.20\,10^{-5}$	60	$1.01\,10^{3}$	$1.07\,10^{-1}$
1/20	42	$4.57\,10^{2}$	$1.27\,10^{-6}$	81	$5.00\,10^{2}$	$2.92\,10^{-6}$	120	$2.09\,10^{3}$	$5.55\,10^{-2}$
1/40	82	$1.01\,10^{3}$	$1.48\,10^{-7}$	161	$1.04\,10^{3}$	$2.40\,10^{-7}$	240	$4.27\,10^{3}$	$2.82\,10^{-2}$

Table 8: Example 4: comparison between IGA-SGBEM, C-SGBEM, S-SGBEM, based on quadratic piecewise polynomial basis functions, for different values of h.

		Galerkin IGA-BEM			collocation IGA-BEM		
h	DoF	cond.	$E_M(h)$	$\log_2\left(\frac{E_M(2h)}{E_M(h)}\right)$	cond.	$E_M(h)$	$\log_2\left(\frac{E_M(2h)}{E_M(h)}\right)$
1/5	12	$7.19\,10^{1}$	$4.03\,10^{-4}$	–	$1.73\,10^{1}$	$4.88\,10^{-4}$	–
1/10	22	$1.87\,10^{2}$	$2.11\,10^{-5}$	4.26	$3.63\,10^{1}$	$5.74\,10^{-5}$	3.09
1/20	42	$4.57\,10^{2}$	$1.27\,10^{-6}$	4.05	$7.70\,10^{1}$	$6.94\,10^{-6}$	3.05
1/40	82	$1.01\,10^{3}$	$1.48\,10^{-7}$	3.10	$1.58\,10^{2}$	$8.58\,10^{-7}$	3.01
1/80	162	$2.12\,10^{3}$	$1.81\,10^{-8}$	3.03	$3.20\,10^{2}$	$1.07\,10^{-7}$	3.00

Table 9: Example 4: comparison between Galerkin and collocation IGA-BEM results, varying h.

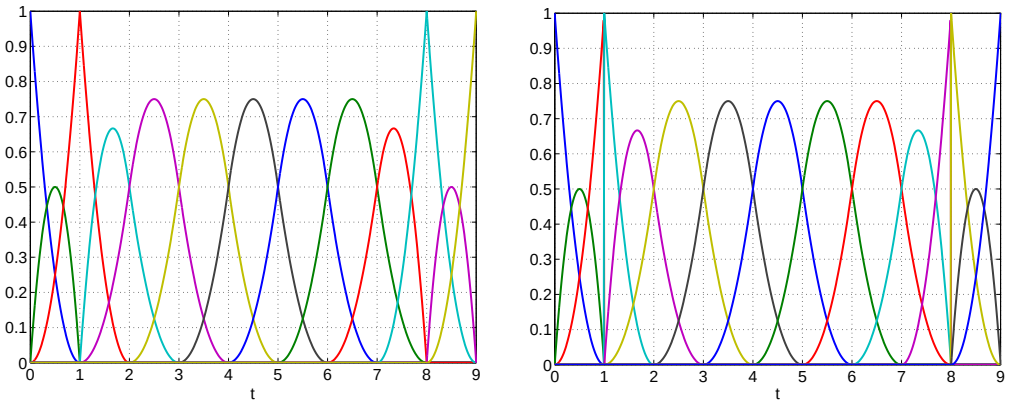

Figure 1: Quadratic B-splines basis with knot vector T_1 (left), and knot vector T_2 (right), related to the same partition of the interval $[0, 9]$.

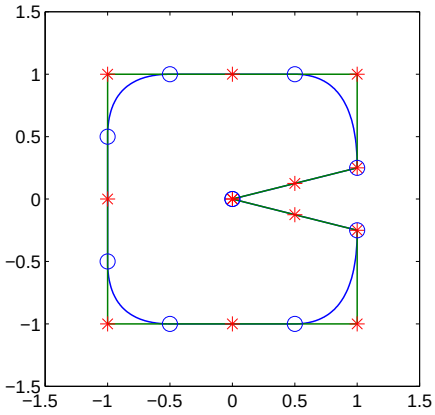

Figure 2: Example 1: the quadratic closed spline curve defining the boundary of the considered interior domain along with the related B-spline control polygon. The control points and the nodal (mesh) points of the spline curve are respectively marked with the symbol '$*$' and '$\circ$'.

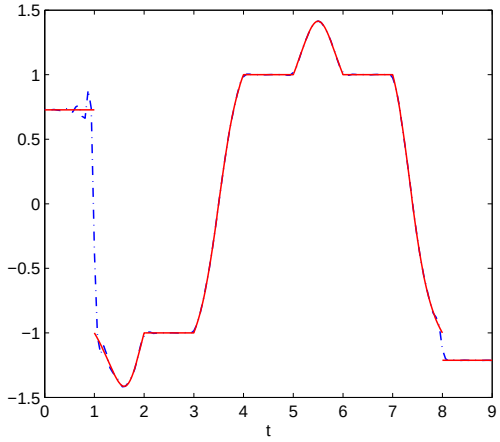

Figure 3: Example 1: the analytical solution (solid) and the numerical solution (dash-dotted), obtained after three refinements of T_1 ($h = 1/8$).

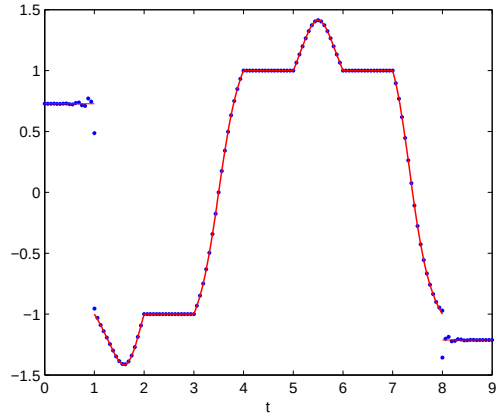

Figure 4: Example 1: the analytical solution (solid) and the numerical solution (dotted), obtained after three refinements of T_2 ($h = 1/8$).

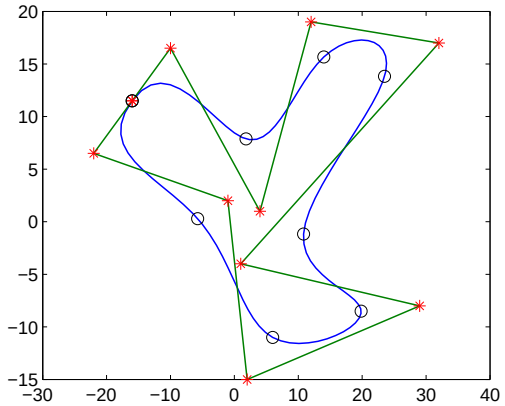

Figure 5: Example 2: the cubic closed spline curve defining the boundary of the considered interior domain along with the related B-spline control polygon. The control points and the nodal (mesh) points of the spline curve are respectively marked with the symbol '$*$' and '$\circ$'.

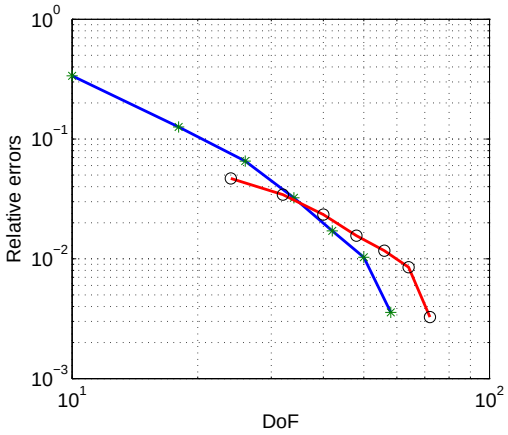

Figure 6: Example 2: relative errors of Table 3 vs DoF with $h = 1/8$ ('$*$' B-splines, '$\circ$' Lagrangian basis).

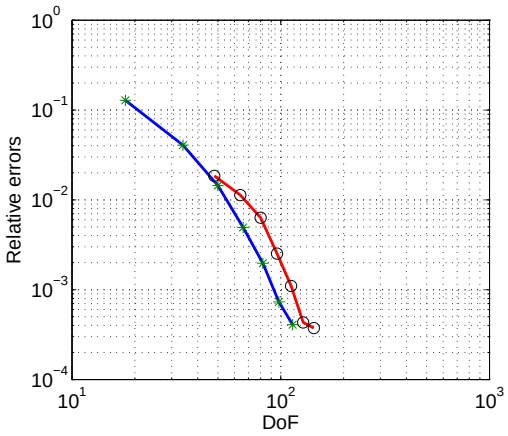

Figure 7: Example2: relative errors of Table 4 vs DoF with $h = 1/16$ ('$*$' B-splines, '$\circ$' Lagrangian basis).

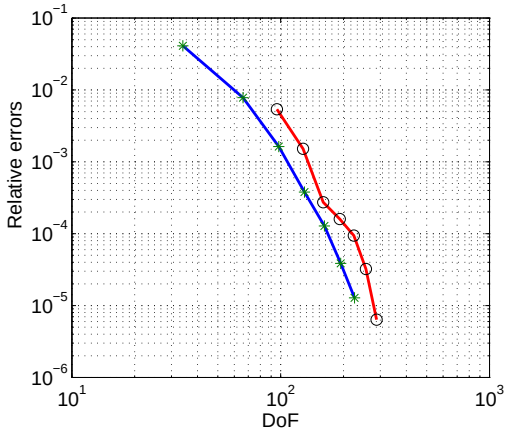

Figure 8: Example 2: relative errors of Table 5 vs DoF with $h = 1/32$ ('$*$' B-splines, '$\circ$' Lagrangian basis).

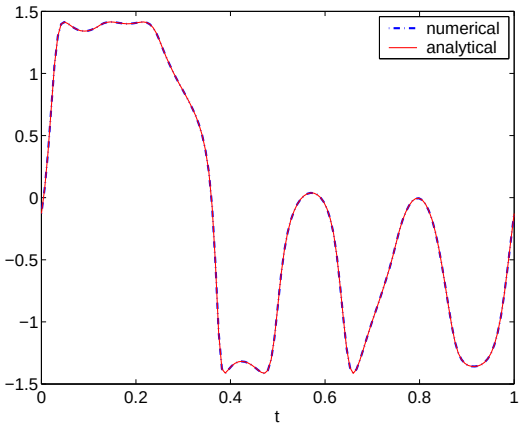

Figure 9: Example 2: approximate solution obtained with the B-spline basis of degree 9 and $h = 1/16$, together with the analytical solution.

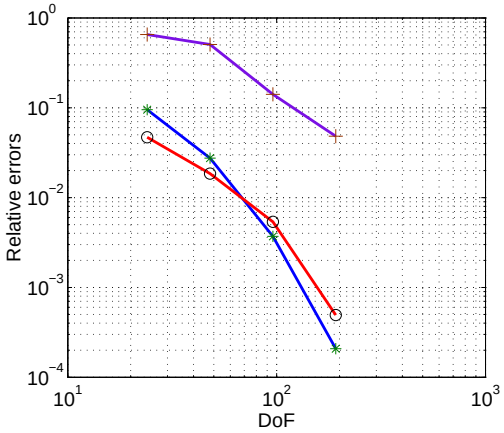

Figure 10: Example 2: relative errors of Table 7 ('$*$' IGA-SGBEM, '$\circ$' C-SGBEM, '$+$' S-SGBEM).

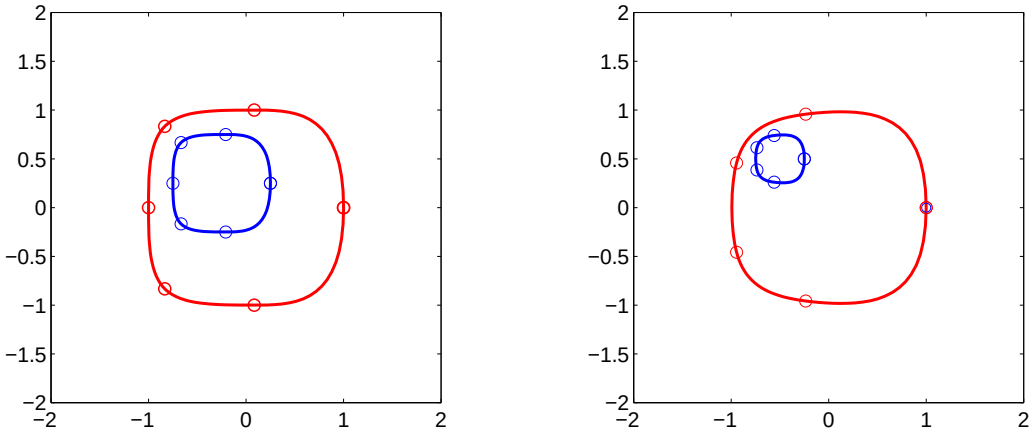

Figure 11: Example 3: Domains with holes. The two closed boundary curves on the left (A) are cubics and those on the right (B) are quartics. The nodal (mesh) points of the spline curves are marked with the symbol '$\circ$'.

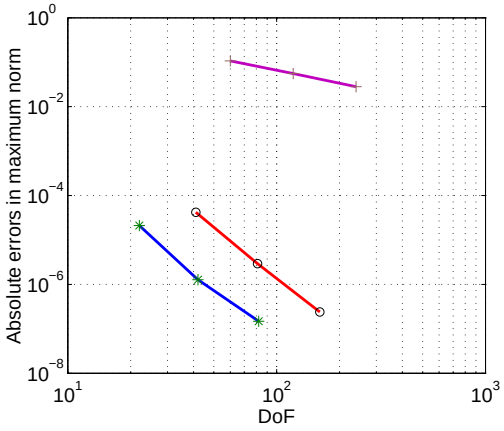

Figure 12: Example 4: Absolute errors, related to quadratic basis functions, for different value of h ('$*$' C^1 B-splines, '$\circ$' C^0 Lagrangian basis, '+' L^2 Lagrangian basis on $\tilde{\Gamma}_h$).